

**KOMATIITES AS MERCURY SURFACE ANALOGUES: SPECTRAL MEASUREMENTS AT PEL.** Alessandro Maturilli<sup>1</sup>, Jörn Helbert<sup>1</sup>, James W. Head<sup>2</sup>, William M. Vaughan<sup>2</sup>, Mario D'Amore<sup>1</sup>, James St. John<sup>3</sup>  
<sup>1</sup>Institute for Planetary Research, German Aerospace Center DLR, Rutherfordstr. 2, Berlin-Adlershof, Germany ([alessandro.maturilli@dlr.de](mailto:alessandro.maturilli@dlr.de)). <sup>2</sup>Department of Geological Sciences, Brown University, Providence, RI 02912, USA. <sup>3</sup>School of Earth Sciences, The Ohio State University at Newark, Newark, OH 43055, USA.

**Introduction:** X-ray fluorescence and gamma ray measurements by the NASA MESSENGER spacecraft orbiting Mercury show a surface composition strongly different from other terrestrial planets [1, 2]. The X-Ray Spectrometer (XRS) measures elemental composition for the topmost 0.1 mm of Mercury's regolith, while the Gamma Ray and Neutron Spectrometer (GRNS) is sensitive to depths of tens of centimeters. High Mg/Si and low Al/Si and Ca/Si ratios exclude a feldspathic surface composition like that of the lunar highlands. Mercury's surface mineralogy is likely dominated by magnesian orthopyroxene, sodium-rich plagioclase feldspar, and lesser amounts of Ca, Mg, and/or Fe sulfides. Enstatite chondrite melts and certain enstatite achondrites provide a good compositional and mineralogical match for much of the surface of Mercury [3]. Elemental results from the GRNS [4] are consistent with those previously obtained by the X-Ray Spectrometer, including the high sulfur and low iron abundances. The elemental results from gamma-ray and X-ray spectrometry are most consistent with petrologic models suggesting that Mercury's surface is dominated by magnesian silicates [5]. Mercury's magnesian silicates and high Mg/Si ratio (in excess of the Mg/Si ratio of terrestrial and lunar basalts [1]) invites comparison to the terrestrial ultramafic lavas known as komatiites.

To assess komatiites as analogs for the surface of Mercury, at the Planetary Emissivity Laboratory (PEL) at the German Aerospace Center (DLR) we have measured visible and infrared spectra for a suite of komatiite samples under a range of environmental conditions.

**Komatiite samples:** We used 3 terrestrial samples from Africa (Barberton, Belingwe, Comondale) and a synthetic one produced at the Brown University Department of Geological Sciences. The Barberton material is an olivine spinifex komatiite from the Paleoproterozoic-aged (3.481 Ga) Lower Komati Formation in the Komati River Valley area, South Africa. This is the type locality, known for the best-preserved very old komatiites on Earth. Unfortunately, the sample has been metamorphosed into black serpentinite, changing its mineralogy [6]. We thus obtained samples of the remarkably fresh Belingwe komatiite [7], another olivine spinifex komatiite, which contains unaltered olivine and glass. Olivine spinifex komatiites such as Barberton and Belingwe contain nearly 10 wt. % FeO,

probably >10 times the concentration of FeO on Mercury's surface [1]. High FeO renders these komatiites suspect as a Mercury spectral analog; moreover, the high (Fe+Mg)/Si of these komatiites suggests an olivine-dominated mafic mineralogy, not the orthopyroxene-dominated mineralogy suggested for Mercury [5]. We thus obtained samples of the low-FeO (~4 wt. % FeO), pyroxene-normative Comondale komatiite [8]. Unfortunately, this komatiite has also undergone substantial alteration; for the perfect analog, a "synthetic komatiite" displaying orthopyroxene spinifex was created by slowly cooling a bulk composition based on XRS measurements (flare #5 of [1]) in an elongated graphite capsule.

**The PEL:** The Bruker VERTEX 80V Fourier Transform Infrared-Spectrometer (FTIR) is operated under vacuum to remove atmospheric features from the spectra. A Bruker A513 accessory is used to obtain biconical reflectance with variable incidence angle  $i$  and emission angle  $e$  between 13° and 85° at room temperature, under purge or vacuum conditions, in the 1 to 100  $\mu\text{m}$  spectral range. The other Bruker IFS 88 has an attached emissivity chamber for measurements at low to moderate temperatures [9, 10]. A Harrick Seagull<sup>TM</sup> variable-angle reflection accessory allows measurement of the biconical reflectance of minerals at room temperature, under purging conditions in the extended spectral range from 0.4 to 55  $\mu\text{m}$ .

**Komatiite spectra:** We handled our natural komatiite samples following our standard procedures: we crushed the bulk rocks into smaller particles, then sieved them to four PEL typical particle size ranges. The synthetic sample was ground by hand to fine dust.

The visible and infrared biconical reflectance spectra for all the samples were measured at room temperature in a purged environment with the Bruker IFS 88 instrument and the the Harrick Seagull<sup>TM</sup> variable-angle reflection accessory. The visible spectral range (VIS, 0.45–1.1  $\mu\text{m}$ ) was sampled with a Si-diode detector and a quartz beamsplitter. For the mid-infrared range (MIR, 1.5–16  $\mu\text{m}$ ), a nitrogen-cooled MCT detector and a KBr beamsplitter were used. We chose illumination angles  $i = e = 40^\circ$  to agree with most of the observations from the MESSENGER Mercury Atmospheric and Surface Composition Spectrometer (MASCS). The samples were poured into stainless steel cups, reflectances measured in the VIS and MIR spectral ranges, then each cup was heated in vacuum

( $10^{-4}$  bar) to  $500^{\circ}\text{C}$  for one hour (T processed), cooled in vacuum to room temperature, and the VIS and MIR reflectances measured again.

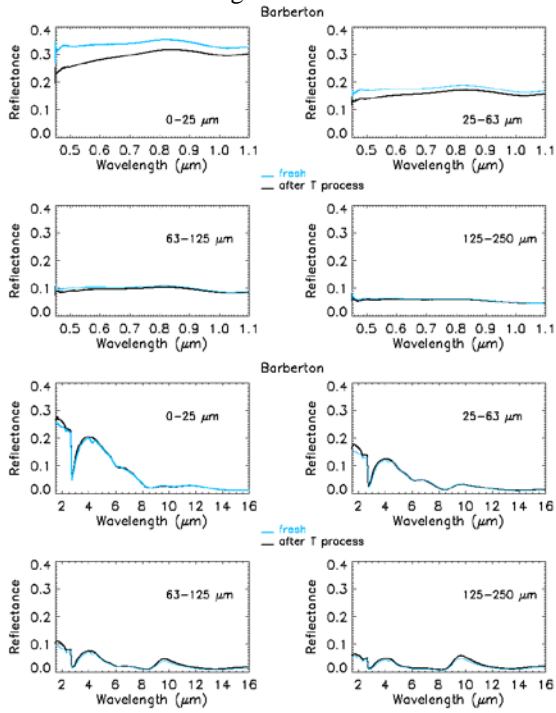


Figure 1. Visible (upper panel) and infrared (lower panel) biconical reflectance spectra ( $i = e = 40^{\circ}$ ) of Barberton komatiite in four PEL grain-size fractions.

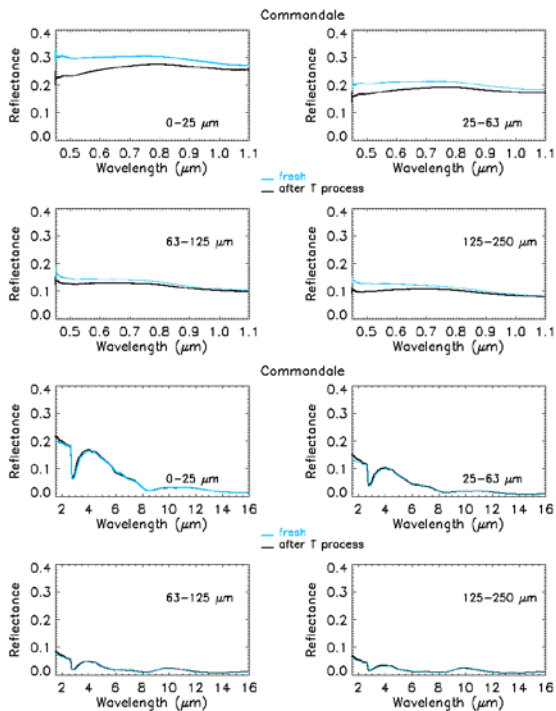


Figure 2. VIS (upper panel) and MIR (lower panel) biconical reflectance spectra ( $i = e = 40^{\circ}$ ) of Comondale komatiite in four PEL grain-size fractions.

In Fig. 1 the VIS and MIR spectra (fresh and after T processing) for the 4 PEL separates of the Barberton sample are shown. In the VIS spectral range, spectral changes between fresh and T processed samples depend on grain size, with greater changes for the finer samples (Mercury more relevant particles); in the MIR range changes are more homogeneous. However, for the Comondale sample (Fig. 2), the trend for the VIS part is inverted at larger grain sizes, while in the MIR little or no changes are observed. In the case of synthetic komatiite (Fig. 3), substantial spectral changes are observed in both channels.

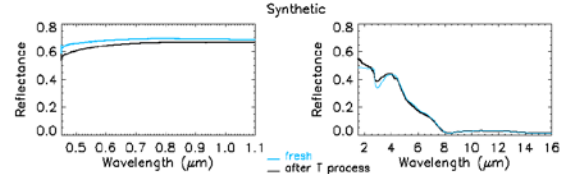


Figure 3. VIS (right) and MIR (left) biconical reflectance spectra ( $i = e = 40^{\circ}$ ) of the Brown Univ. synthetic komatiite.

**Summary:** We have measured visible and infrared reflectance spectra for a suite of natural and synthetic komatiite samples, before and after heating to  $500^{\circ}\text{C}$ , with illumination angles matching most of MASCs observations. Samples after T processing show changes in both the VIS and MIR. However, changes in the VIS are stronger, with reddening occurring with all samples; some samples darkened. Effects of T processing are not systematic: we infer a dependence on chemical composition/crystallinity of the samples. Previous experiments on repeated heating and cooling of komatiites show that the spectral changes from T processing are cumulative [11].

Collectively, these measurements can provide support to the analysis of MESSENGER spectral reflectance data [e.g., 12]. They also might help to test the hypothesis that hollows form in magnesian crust in the course of removal of surficial sulfide deposits [13,14].

**References:** [1] Nittler L. R. et al. (2011) *Science*, 333, 1847. [2] Peplowski P. N. et al. (2011) *Science*, 333, 1850. [3] Weider S. Z. (2012) *JGR*, 107, E10. [4] Evans L. G. (2012) *JGR*, 107, E10. [5] Stockstill-Cahill, K. R. et al. (2012) *JGR*, 107, E10. [6] Parman S. W. et al. (1997) *EPSL* 150, 303. [7] Nisbet, E. G. et al. (1987), *Geology*, 15, 1147-1150. [8] Williams, D. A. et al. (1999), *LPSC*, 30. [9] Maturilli A. et al. (2006) *PSS*, 54, 1057. [10] Maturilli A. et al. (2008) *PSS*, 56, 420. [11] Maturilli A. et al. (2012), *LPS*, XXXIII, Abstract #1394. [12] D'Amore M. et al. (2013), *LPS*, XXXIV, this meeting. [13] Helbert J. et al. (2013), *LPS*, XXXIV, this meeting. [14] Vaughan, W. M. et al. (2012), *LPS*, XXXIII, Abstract #1187.